Research Article

Application of 3D QSAR CoMFA/CoMSIA and *In Silico* Docking Studies on Potent Inhibitors of Interleukin-2 Inducible T-cell Kinase (ITK)

Shravan Kumar Gunda*, Sri Swathi Mutya, Sharada Durgam, Swarna Adepu, Mahmood Shaik
Bioinformatics Division, Osmania University, Hyderabad, Andhra Pradesh, India.
***Corresponding author's E-mail:** gunda14@gmail.com

Accepted on: 16-10-2014; **Finalized on:** 31-12-2014.

ABSTRACT

Computational chemistry is playing an immensely important role in drug design, discovery and QSAR studies. Interleukin-2 inducible T-cell kinase is a member of the Tec kinase family which plays an important role in T-cell development and activation and proliferation and also the modulation of T-cells they are selected for the discovery of potent inhibitors of ITK through ligand and structure-based drug design. The conventional ligand-based 3D-QSAR studies were performed based on the lower energy conformations using SYBYL database alignment rule. The ligand based model gave q^2 values of 0.718 and 0.632, r^2 values of 0.977 and 0.978 for CoMFA and CoMSIA. The models were efficiently able to predict the activity of test set molecules within acceptable error range. In silico molecular docking studies were performed by using FlexX. The data rendered from 3D-QSAR study provided insight to design novel potential ITK inhibitors.

Keywords: 3D-QSAR, CoMFA, CoMSIA, Interleukin-2 inducible T-cell Kinase, FlexX

INTRODUCTION

ITK (Interleukin-2-inducible T-cell kinase) is an important member of the TEC family of non-receptor tyrosine kinases expressed in T-lymphocytes, NK cells and mast cells[1] which is activated on ligation of the T-cell receptor (TCR), CD3, and CD28. ITK plays an important role in T-cell development and activation and proliferation[2].

The TEC family of non-receptor tyrosine kinases, including ITK2 is the 2nd largest family of non-receptor tyrosine kinases[3].

Interleukin-2-inducible T-cell kinase is structurally organized into 5 domains, an N-terminal pleckstrin homology domain, followed by a TEC Homology domain with a proline-rich region[4] which contains a Zn^{2+} binding BH motif and one PRR, a SH3 domain, and SH2 domains, and a C-terminal kinase domain. They regulate signals produced from multiple receptors[5], most importantly the BcR and TcR.[6,7]

ITK in particular has been shown to regulate TcR signals leading to increases in intracellular calcium.[8,9] extracellular signal regulated kinase, activation of transcription factors AP1, NFAT and mitogen activated protein kinase. During stimulation of the T cell receptor, PI3K is activated, resulting in the formation of cell membrane phosphoinositides, to which the pleckstrin homology domain of ITK binds.

Interleukin-2-inducible T-cell kinase also forms dimers specifically at the plasma membrane in the proximity of receptors that activate phosphatidylinositol 3-kinase[10].

Upon activation, ITK is enriched in membrane rafts and interact with other signalling proteins through its SH2, SH3, and TH domain. In the recent time, it has been proved that ITK regulates the secretion of Th2 cytokines. In addition to this ITK has been shown to be involved in the development of conventional phenotype $CD8^+$ T cells, $CD4^+$ T cells and Natural killer cells[11-13].

In this study, by using 3D-QSAR and molecular docking analyses it is possible to get new insights into the relationship between the structural information of the series of 46 ITK inhibitory compounds, with the aim of identifying structural features in ITK that can be used to find new inhibitors.

Computational Details

Molecular Structures and Optimization

Forty six molecules selected for the present study were taken from an earlier report[14] and were manually drawn using Tripo's Sybyl 6.7 software.[15]

These molecules were minimized using Gasteiger-Huckel charges[16] after adding hydrogen's to their most appropriate conformation using Powell method after which they were added to a database for carrying out 3D QSAR, CoMFA[17] CoMSIA and docking studies.

The compound structures and their biological activities are given in Table 1 and 2.

The IC_{50} values of the compounds were converted to pIC_{50} by taking $-\log IC_{50}$ values and used as dependent variables in CoMFA and CoMSIA[18].

Out of the 46 compounds taken into the study 3D-QSAR models were generated using a training set of 37 molecules and predictive power of the resulting models was evaluated using a test set of 9 molecules.

The compounds in the test set were selected randomly.

Table 1: Compound Structures

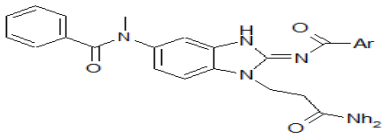

Compound No	Ar
1	Phenyl
2	4-Cl-phenyl
3	4-CN-phenyl
4	4-OMe-phenyl
5	4-Br-phenyl
6	3-Biphenyl
7	1-Naphthyl
8	2-Naphthyl
9	2-Thiophene
10	3-Thiophene
11	4-Thiazole
12	5-Thiazole
13	2-Oxazole
14	4-Oxazole
15	5-Oxazole
16	5-Isoxazole

Table 2: Compound Structures

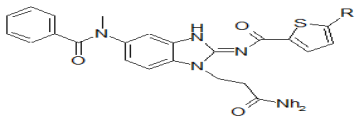

Compound No	R
17	Cl
18	Br
19	CN
20	CHO
21	COCH3
22	COCH(CH3)2
23	COPh
24	OPh
25	Obn
26	Ph
27	2-Pyr
28	3-Pyr
29	4-Pyr
30	**2-Oxazole**
31	4-Oxazole
32	5-Oxazole
33	2-Me-5-oxazole
34	2-Thiazole
35	2-Amino-4-Thiazole
36	4-Pyrazole
37	2-Pyrazine
38	Pyrrolidine
39	Piperidine
40	Piperazine
41	4-Morpholine
42	2-CN-4-pyridine
43	2-F-4-pyridine
44	2-CN-5-Pyridine
45	2-F-5-pyridine
46	3-CN-5-pyridine

Molecular Alignment based on a Common Scaffold

Molecular alignment is the most sensitive parameter in 3D-QSAR analyses. The quality and predictive power of the model were directly dependent on the alignment rule.[19] CoMFA results are sensitive to a number of factors such as alignment, lattice shifting step size and probe atom type. Structural alignment plays an important role in the prediction of CoMFA models and the reliability of these contour models depend strongly on the structural alignment of the molecules taken into study.[20] Molecular alignment was achieved by SYBYL routine align database. The most active compound 46 was used as a template to align the rest of the compounds from the series by common substructure alignment, using the ALIGN DATABSE command in Sybyl 6.7. The scaffold structure used for alignment and all molecules superimposed based on that scaffold after alignment is represented in Figure 1.

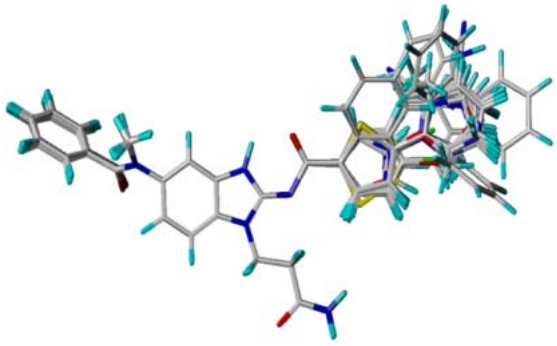

Figure 1: 3D-view of aligned molecules (training and test sets) based on SYBYL alignment method.

Comparative Molecular Field Analysis

In CoMFA[21] steric and electrostatic fields were calculated using the Lennard-Jones and Coulomb potentials with a distance dependent dielectric constant at all interactions in a regularly spaced (2Å) grid taking a sp^3 carbon atom as steric probe and a+1 charge as electrostatic probe.[22] The cut-off value was set to 30 Kcal/mol. Using default scaling of variables, regression analysis (r^2) was carried out using fully cross-validated partial least squares (PLS) method (leave one out/LOO).[23] The column filtering parameter was set to 2.0 Kcal/mol to improve the signal to noise ratio by omitting those lattice points whose energy variation was below this threshold.

Comparative Molecular Similarity Indices Analysis

CoMSIA approach is a substitution to perform 3D-QSAR by CoMFA. Molecular similarity is evaluated in similarity indices terms. In CoMSIA a distance-dependent Gaussian-type physicochemical function has been adopted to avoid uniqueness at the atomic positions and dramatic changes of potential energy for those grids in the proximity of the surface.

The CoMSIA[24] method specifies explicit steric, electrostatic along with hydrophobic, hydrogen bond donor and acceptor fields which were calculated using

the sp^3 carbon probe atom with a+1 atom charge and 1.0 Å radius.[25] In CoMFA only steric and electrostatic fields were calculated. Primarily, the intention is to divide different properties into various placements where they play a decisive role in determining the biological activity. In general, similarity indices, AF, K between the compounds of interest were computed by placing a probe atom at the intersections of the lattice points using below equation.

$$A^{q}_{F,K}(j) = \sum_{i=1}^{n} W_{probe,k} W_{ik} e^{-a r^2_{iq}}$$

Where 'A_F' is the similarity index, 'q' is a grid point, 'i' is a summation index over all atoms of the molecule 'j' under computation, 'W_{ik}' is actual value of the physicochemical property 'k' of atom 'I'; '$W_{probe,\ k}$' is value of the probe atom and the mutual distance between the probe atom at grid point q and atom i of the test molecule is represented by 'r_{iq}'. In the present study, similarity indices were computed using a probe atom ($W_{probe,\ k}$) with charge +1, radius 1 Å, hydrophobicity +1, and attenuation factor a of 0.3 for the Gaussian type distance. The statistical valuation for the CoMSIA analyses was performed in the same manner as described for CoMFA.

Partial Least Square (PLS) Analysis

Partial least square analysis is used to correlate ITK inhibitor activities with the CoMFA and CoMSIA values. The predictive value of the models was evaluated first by leave-one-out (LOO) cross-validation method in which one compound is removed from the dataset and its activity is predicted by using the model derived from the rest of the molecules in the dataset. A minimum column filtering value of 2.0 Kcal mol^{-1} was used for the cross-validation to speed up the analysis and to reduce the signal-to-noise ratio. The cross-validated coefficient 'q^2' was calculated according to the following equation:

$$q^2 = 1 - \frac{\sum (Y_{pred} - Y_{actu})^2}{\sum (Y_{actu} - Y_{mean})^2}$$

Where Y_{pred}, Y_{actu} and Y_{mean} are predicted, actual and mean values of the target property (pIC_{50}), respectively; and

$$\sum (Y_{actu} - Y_{mean})^2 = PRESS$$

PRESS is the prediction error sum of the squares, derived from the LOO method. The ONC (optimum number of components) corresponding to the lowest PRESS value was used for deriving the final partial least square regression models. By using the same number of components performed the non-cross-validation to calculate conventional r^2 (regression analysis).

Molecular Docking using Sybyl FlexX Docking Suit

Docking studies were carried out using the FlexX program interfaced with SYBYL6.7. In this automated docking program, the flexibility of the ligands is considered while the protein or biomolecule is considered as a rigid structure. The ligand is built in an incremental fashion, where each new fragment is added in all possible positions and conformations to a pre-placed base fragment inside the active site.[26]

All the molecules for docking were sketched in the SYBYL and minimized are using Gasteiger-Huckel charges. The 3D coordinates of the active sites were taken from the X-ray crystal structure.

The active site was defined as the area within 6.5 A°. After completion of docking active site and ligand were loaded using FlexX browse results options.

Then the hydrogen bond interactions between the receptors and ligand were checked.

RESULTS AND DISCUSSION

3D-QSAR Model Validation

CoMFA and CoMSIA 3D-QSAR models were derived using ITK inhibitors. The 9 randomly selected compounds were used as test set and 37 compounds were used as training set to maintain the stability and predictive ability of the CoMFA and CoMSIA models (see Table 3 for training set and test set molecules).

The predicted pIC_{50} with the quantitative structure activity relationship models are in good agreement with the experimental data within a statistically adequate error range.

CoMFA Analysis

37 compounds out of the 46 ITK inhibitors were used as training set and 9 compounds were used as test set. The test set compounds were selected randomly so that the structural diversity and wide range of activity in the dataset were included.

PLS analysis was carried out for the training set and a cross-validated 'q^2' of 0.718 for five components was obtained.

The non cross-validated PLS analysis with the optimum components revealed a conventional 'r^2' value of 0.977, F value = 263.037 and an estimated standard error of estimate (SEE) of 0.137.

The steric field descriptors contribution is 62.4% of the variance, while the electrostatic field contribution is 37.6% of the variance. 100 runs were carried out for Bootstrap analysis for further validation of the model by statistical sampling of the original dataset to create new datasets.

This yielded higher r^2 bootstrap value of 0.987 conforming the statistical validity of the developed models. Figure 2 represents the correlation between the predicted and the experimental values.

The predicted activities using the CoMFA model are in good agreement with the experimental data, suggesting

that the CoMFA model should have a satisfactory predictive ability.

Results show that prediction by the CoMFA model is reasonably accurate.

Table 3: Compounds used in Training set and Test set; *Bold indicates Test set

C.NO	pIC_{50} values	CoMFA		CoMSIA		Dock score
		Predicted	Residual	Predicted	Residual	
1	6.74	6.78	-0.04	6.91	-0.17	-26.3
2	**7.74**	**7.34**	**0.40**	**7.32**	**0.42**	**-26.4**
3	7.76	8.23	-0.47	7.84	-0.08	-26.9
4	6.76	6.22	0.54	6.50	0.26	-25.5
5	7.58	7.07	0.51	6.97	0.61	-26.4
6	6.00	6.08	-0.08	6.02	-0.02	-27.0
7	5.60	6.23	-0.63	6.29	-0.69	-32.4
8	**7.02**	**6.71**	**0.31**	**6.52**	**0.50**	**-27.7**
9	**7.3**	**6.60**	**0.70**	**7.16**	**0.14**	**-25.4**
10	**7.24**	**6.51**	**0.73**	**7.01**	**0.23**	**-25.5**
11	6.46	6.81	-0.35	6.52	-0.06	-28.9
12	6.88	6.91	-0.30	6.93	-0.05	-28.9
13	6.34	6.74	-0.4	7.17	-0.83	-25.4
14	6.76	6.69	0.07	6.97	-0.21	-28.4
15	6.74	6.91	-0.17	7.19	-0.45	-29.8
16	7.00	6.65	0.35	6.32	0.68	-32.1
17	7.85	7.74	0.11	7.72	0.13	-25.5
18	7.82	7.95	-0.13	7.74	0.08	-26.1
19	**7.82**	**8.60**	**-0.78**	**8.04**	**-0.22**	**-25.8**
20	8.69	8.01	0.68	8.39	0.30	-28.4
21	7.85	8.41	-0.56	8.12	-0.27	-30.4
22	7.69	8.20	-0.51	8.10	-0.41	-34.0
23	7.25	6.94	0.31	7.15	0.10	-31.8
24	6.85	7.12	-0.27	7.09	-0.24	-29.2
25	7.45	8.14	-0.69	7.27	0.18	-24.6
26	**7.40**	**8.34**	**-0.94**	**7.87**	**-0.47**	**-27.8**
27	**7.72**	**8.13**	**-0.41**	**7.73**	**-0.01**	**-28.8**
28	8.30	8.26	0.04	8.44	-0.14	-27.9
29	8.69	7.89	0.80	8.60	0.09	-27.5
30	8.09	8.30	0.21	8.35	-0.26	-26.9
31	7.85	7.88	-0.03	8.00	-0.15	-27.1
32	8.69	8.78	-0.09	8.62	0.07	-32.1
33	8.22	8.57	-0.35	8.40	-0.18	-26.1
34	**7.95**	**8.32**	**-0.37**	**8.33**	**-0.38**	**-27.5**
35	8.00	8.04	-0.04	7.90	0.10	-28.1
36	8.69	7.78	0.91	8.18	0.51	-33.6
37	**7.88**	**8.38**	**-0.5**	**8.60**	**-0.72**	**-31.2**
38	7.09	6.95	0.14	6.81	0.28	-28.9
39	6.42	6.97	-0.55	6.98	-0.56	-27.1
40	6.82	7.07	-0.25	6.91	-0.09	-26.3
41	7.13	6.84	0.29	7.62	-0.49	-31.1
42	8.09	8.32	-0.23	8.27	-0.18	-29.3
43	8.52	8.28	0.24	8.28	0.24	-32.4
44	8.00	8.08	-0.08	7.98	0.02	-28.1
45	8.30	8.35	-0.05	8.12	0.18	-32.3
46	8.69	8.44	0.25	8.09	0.60	-28.8

CoMSIA Analysis

The CoMSIA analyses were performed using five descriptor fields: steric, electrostatic, hydrophobic, hydrogen bond donor and acceptor. The CoMSIA study disclosed a cross validated q^2 of 0.632 with an optimum number of components as 6, a conventional r^2 of 0.978 with a standard error of estimate 0.137 and F value 220.813 was obtained. The steric field contribution 13.0 % of the variance and the electrostatic descriptor explains 28.3 %, the hydrophobic field explains 19.8% while the hydrogen bond donor explains 27.8 % of the variance and hydrogen bond acceptor field contribution is 11.1%. For Bootstrap 100 runs was then carried out for model validation by statistical sampling of the original dataset to create new datasets. This yielded higher r^2 bootstrap value of 0.989 affirming the statistical validity of the developed models. The predicted activities are given in Table 4

Table 4: Statistical Analysis of CoMFA and CoMSIA Models.

Field Name	CoMFA		CoMSIA	
q^2	0.718		0.632	
r^2	0.977		0.978	
Standard Error of Estimate	0.137		0.137	
F value	263.037		220.813	
Cross Validation	0.713		0.617	
Bootstrap	Mean	Std. dev	Mean	Std. dev
SEE	0.103	0.065	0.094	0.065
r^2	0.987	0.005	0.989	0.006
Field Contributions				
Steric	62.4%		13.0%	
Electrostatic	37.6%		28.3%	
Hydrophobic	-		19.8%	
Donor	-		27.8%	
Acceptor	-		11.1%	

Correlation between the experimental and predicted bioactivities was shown in Figure 2(a) and 2(b).

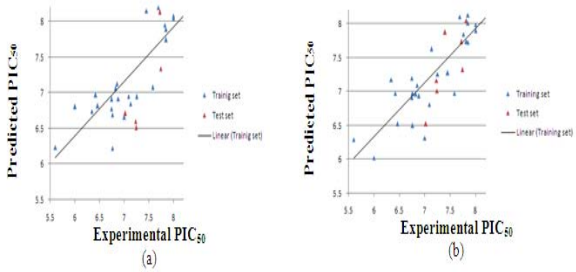

Figure 2: Predicted and observed activities of training and test sets using (a) CoMFA and (b) CoMSIA models

Contour Analysis

To estimate the field impact on the target property, CoMFA and CoMSIA isocontour diagrams were produced. The isocontour diagrams are used to identify the

important regions where changes can be made in the steric, electrostatic, hydrophobic, hydrogen-bond donor, and acceptor fields which may affect the biological activity. Additionally, these diagrams may be beneficial in discovering important characteristics of the ligand and receptor interactions. The field energies of all fields were calculated with the weight of the standard deviation and the coefficient. In Figures 3 and 4, the isocontour diagrams obtained from the CoMFA and CoMSIA are interpreted together with template ligand. These maps show the regions where modification of compounds field properties led to an increase or decrease in the pIC_{50} value.

CoMFA Contour Analysis

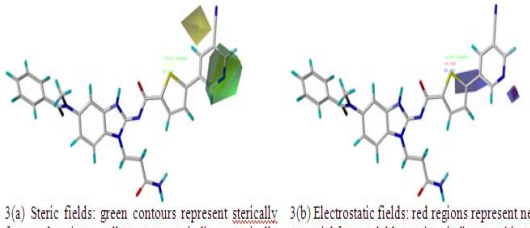

3(a) Steric fields: green contours represent sterically favoured regions; yellow contours indicate sterically disfavoured regions.

3(b) Electrostatic fields: red regions represent negative potential favoured; blue regions indicate positive charge favoured.

The CoMFA steric contours derived from the inhibitory activities of ITK inhibitors shown below in Figure 3, and as detailed above the green coloured isopleth region present at 3-CN-5-Pyridine ring at the para position in the contour map of the highest active molecule 46 (pIC_{50}= 8.69) indicated that substitution at this positions with bulky steric group favours and enhances the ITK inhibitory activity of the molecule where as the yellow isopleths shows areas where bulky steric group substitutions are disfavoured and ought to be circumvented in order to enhance the activity of ITK inhibition.

The CoMFA electrostatic contours derived for the same highest active compound 46 is displayed in Figure 3 and from the figure it can be clearly seen that the more electropositive substituent's at the are blue isopleth regions at the ortho position of the phenyl ring is favoured for enhancing the activity of the molecule whereas red isopleth at the para position of the 3-CN-5-Pyridine position of the phenyl ring favours more electronegative substitutions for enhancing the ITK inhibitory activity.

CoMSIA Contour Analysis

The steric and electrostatic CoMSIA contours of the most active molecule depicted in Figure 4a and 4b are comparable to the CoMFA contours and perhaps are better explanatory than the latter. In steric CoMFA contours, we observed the presence of a prominent green isopleth at the para position of the 3-CN-5-Pyridine ring; similar green contour is also present in the CoMSIA steric map indicating that by substituting a bulky steric group at this place will favourably increase the ITK inhibitory activity of the molecule. In CoMFA map we could observe the presence of green and yellow contours near the phenyl ring which are not prominent, but in CoMSIA map of the same we can clearly see these isopleths, the presence of both yellow and green isopleths at the para and meta positions of the 3-CN-5-Pyridine ring indicates the importance of the nitrogen group of phenyl ring rather than any other groups and might indicate the reason for the molecule's high activity.

Like the steric CoMFA–CoMSIA contours, CoMSIA electrostatic contour is also comparable to its Contour part electrostatic CoMFA map, the large red isopleth present at the meta-para position of the 3-CN-5-Pyridine ring in both the maps indicate that substitution at these regions with electronegative groups will favourably increase the molecules ITK inhibitory activity and like the steric CoMFA contours the CoMFA electrostatic contours shows areas of red and blue isopleths which are not comprehensible but whereas the CoMSIA Contour part shows well-defined single blue isopleth at attachment position of 3-CN-5-Pyridine ring suggesting that replacement of these areas with electropositive groups will increase the molecule's ITK inhibitory activity.

Figure 4c represent the hydrophobic CoMSIA contours which are generally denoted in the yellow and white contours representing favourable and unfavourable hydrophobic group substituting regions, and from the figure we can clearly note large white isopleths nearly covering thiophene molecule, indicating that hydrophobic groups substitution in the molecule will drastically decrease its ITK inhibition action but by substituting hydrophilic groups in the molecule can radically increase the molecules ITK inhibition action.

The CoMSIA hydrogen bond acceptor and donor contours are represented in Figure 4d, and as described previously the magenta contours present nearby 3-CN-5-Pyridine position, which indicates that substitution of hydrogen bond acceptor groups at these regions increases the inhibitory activity of the molecule against ITK whereas the red contours present at the sulphur group of Thiophene ring denotes that replacement of these positions with hydrogen bond acceptor groups will significantly decrease the molecule's inhibitory activity.

Similarly, the cyan contour present nearby at the meta position of the 3-CN-5-Pyridine ring suggests areas of favourable hydrogen bond donor group substitution for increased ITK inhibition but whereas the purple contour parts disfavours the hydrogen bond donor group substitution.

Figure 4e displays the hydrogen-bond acceptor contour maps represented by magenta and red contours.

Magenta contours indicate regions where hydrogen-bond acceptor substituents on ligands can be favored and the red ones represent areas where such substituents on inhibitors may be disfavored.

In both Figure 4e, two red contours present at thiophene ring and a magenta contour visible at 3-CN-5-pyridine ring

which display the importance of the presence of hydrogen-bond acceptor groups for ITK inhibitory activity.

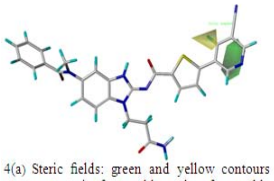

4(a) Steric fields: green and yellow contours represent steric favourable and unfavourable regions respectively.

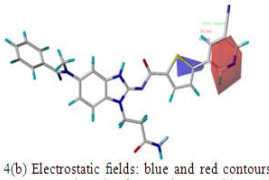

4(b) Electrostatic fields: blue and red contours represent regions that favour electropositive and electronegative groups respectively.

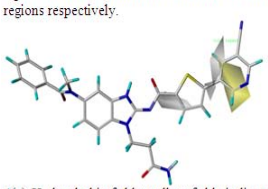

4(c) Hydrophobic fields: yellow fields indicate regions where hydrophobic groups could enhance the activity; while white fields indicate regions where hydrophobic groups decrease activity.

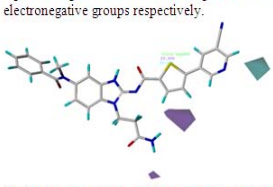

4(d) Hydrogen-bond donor fields: cyan and purple contours represent favourable and unfavourable hydrogen-bond donor regions, respectively.

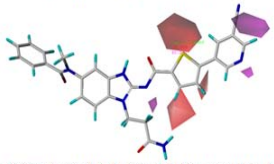

4(e) Hydrogen-bond acceptor fields: magenta and red contours represent favourable and unfavourable hydrogen-bond acceptor regions, respectively.

Molecular Docking

Molecular docking studies were performed by using flexX software, installed on Silicon Graphics Inc octane2 workstation. Crystal structure of ITK inhibitor complex (PDB ID: 3QGY) protein's active site was obtained from PDB database.

The Sybyl software docks the ligands based upon an incremental construction algorithm that coalesce a proficient method for overlap detection and the search for new interactions. For this docking procedure default parameter was used.

Most active compound interacts with Lys391, Ile369 and Met438. Lys391 and Ile369 shows only one interaction with distance of 2.21 and 2.20 respectively. Met438 shows two interactions having distance of 1.52 and 1.74. While least active compound interacts with four amino acids i.e., Lys367, Ile369, Ser371, Met438.

CONCLUSION

3D-QSAR analyses (CoMFA and CoMSIA) were performed with the aim of deriving structural requirements for better ITK inhibitory activity.

3D-QSAR Analysis of this dataset resulted in CoMFA and CoMSIA models with good conventional and cross validated correlation coefficient by field fit method.

Both CoMFA and CoMSIA show that steric and electrostatic fields contribute significantly towards ITK inhibitory activity.

Both the models were able to predict the activity of the test set molecules with good predictive correlation coefficient.

The structural requirement information derived from this 3D-QSAR study could be useful in further designing of potent novel ITK inhibitors.

REFERENCES

1. Readinger JA, Mueller KL, Venegas AM , Horai R, Schwartzberg PL, Tec kinases regulate T-lymphocyte development and function: new insights into the roles of Itk and Rlk/Txk. Immunol Rev, 228, 2009, 93-114.
2. Schwartzberg PL, Finkelstein LD, Readinger JA, TEC-family kinases: regulators of T-helper-cell differentiation. Nat Rev Immunol, 5, 2005, 284-295.
3. Smith CI, Islam TC, Mattsson PT, Mohamed AJ, Nore BF, Vihinen M, The Tec family of cytoplasmic tyrosine kinases: mammalian Btk, Bmx, Itk, Tec, Txk and homologs in other species. Bioessays, 23, 2001, 436-446.
4. Waldmann TA, The structure function and expression of interleukin-2 receptors on normal and malignant lymphocytes. Science. 232, 1986, 727-732.
5. Andreotti AH, Schwartzberg PL, Joseph RE, Berg LJ, T-cell signaling regulated by the Tec family kinase Itk. Cold Spring Harb Perspect Biol, 2, 2010, 2287.
6. August A, Fischer A, Hao S, Mueller C, Ragin M, The Tec family of tyrosine kinases in T cells, amplifiers of T cell receptor signals. Int J Biochem Cell Biol, 34, 2002, 1184-1189.
7. August A, Gibson S, Kawakami Y, Kawakami T, Mills GB, Dupont B, CD28 is associated with and induces the immediate tyrosine phosphorylation and activation of the Tec family kinase ITK/EMT in the human Jurkat leukemic T-cell line. Proc. Natl. Acad. Sci. U.S.A, 91, 1994, 9347-9351.
8. Fowel DJ, Shinkai K, Liao XC, Beebe AM, Coffman RL, Littman DR, Locksley RM, Impaired NFATc translocation and failure of Th2 development in Itk-deficient CD4+ T cells. Immunity, 11, 1999, 399-409.
9. Liu KQ, Bunnell SC, Gurniak CB, Berg LJ, T cell receptor-initiated calcium release is uncoupled from captivative calcium entry in ITK-deficient T cells. J Exp Med, 187, 1998, 1721-1727.
10. Ching KA, Kawakami Y, Kawakami T, Tsoukas CD, Emt/Itk associates with activated TCR complexes role of the pleckstrin homology domain. J Immunol, 163, 1999, 6006-6013.
11. Hu J, Sahu N, Walsh E, August A, Memory phenotype $CD8^+$ T cells with innate function selectively develop in the absence of active Itk. Eur J Immunol, 37, 2007, 2892-2899.
12. Atherly LO, Lucas JA, Felices M, Yin CC, Reiner SL, Berg LJ, The Tec family tyrosine kinases Itk and Rlk regulate the development of conventional CD8+ T cells. Immunity, 25, 2006, 79-91.
13. Broussard C. Fleischecke C, Horai R, Chetana M, Venegas AM, Sharp LL, Hedrick SM, Fowlkes BJ, Schwartzberg PL, Altered development of CD8+ T cell lineages in mice deficient for the Tec kinases Itk and Rlk. Immunity, 25, 2006, 93-104.
14. Brian NC, Bentzien J, Andre W, Nemoto PA, Wang JI, Man CC, Soleymanzadeh F, Khine HH, Kashem MA, Kugler SZ, Wolak JP, Roth GP, Lombaerta SD, Pullen SS, Takahashia H,

Discovery of potent inhibitors of interleukin-2 inducible T-cell kinase (ITK) through structure-based drug design. Bioorganic & Medicinal Chemistry Letters, 19, 2009, 773-777.

15. SYBYL6.7 is available from Tripos Associates Inc, 1699 S. Hanley Rd., St. Louis, MO 631444, USA.
16. Gasteiger JJ, Marsili M, Iterative partial equalization of orbital electro negativity-a rapid process of atomic charges. Tetrahedron, 36, 1980, 3219-3228.
17. Klebe G, Abraham U, Mietzner T, Molecular similarity indices in a comparative molecular field analysis (CoMFA) of drug molecules to correlate and predict their biological activity. J Med Chem, 37, 1994, 4130-4146.
18. Ashok SN, Mayura AK, Tukaram MK, Qsar study on 3-substituted indole derivatives as anti-inflammatory agents, Int J Pharm Bio Sci, 4, 2013, 482–492.
19. Cramer RD, Patterson DE, Bunce JD, Comparative molecular field analysis (CoMFA) 1. Effect of shape on binding of steroids to carrier proteins. J Am Chem Soc, 110, 1988, 5959-5967.
20. Cho SJ, Tropsha A, Cross-validated R^2 region selection for CoMFA. J. Med. Chem, 38, 1995, 1060-1066.
21. Kubinyi H, QSAR and 3D QSAR in drug design. Drug Discov. Today, 2, 1997, 457-467.
22. Xue CX, Cui SY, Liu MC, Hu ZD, Fan BT, 3D QSAR studies on antimalarial alkoxylated and hydroxylated chalcones by CoMFA and CoMSIA. European Journal of Medicinal Chemistry, 39, 2004, 745-753.
23. Bush BL, Nachbar RB, Sample-distance partial least squares: PLS optimized for many variables, with application to CoMFA. J Comput Aided Mol Des, 5, 1993, 587-619.
24. Durdagi S, Kapou A, Kourouli T, Andreou T, Nikas SP, The application of 3D-QSAR studies for novel cannabinoid ligands substituted at the C1' position of the alkyl side chain on the structural requirements for binding to cannabinoid receptors CB1 and CB2. J Med Chem, 50, 2007, 2875-2885.
25. Klebe G, Abraham U, Mietzner T, Molecular similarity indices in a comparative analysis (CoMSIA) of drug molecules to correlate and predict their biological activity. J Med Chem, 37(24), 1994, 4130-4146.
26. Rarey M, Kramer B, Lengauer T, Klebe G, A fast flexible docking method using an incremental construction algorithm. J Mol Biol, 261, 1996, 470-489.

Source of Support: Nil, **Conflict of Interest:** None.